Title
Polychromatic SSVEP stimuli with subtle flickering adapted to brain-display interactions

Journal
Journal of Neural Engineering, 14(1)

ISSN
1741-2560

Authors
Chien, Yu-Yi
Lin, Fang-Cheng
Zao, John K
et al.

Publication Date
2017-02-01

DOI
10.1088/1741-2552/aa550d

Peer reviewed

Polychromatic SSVEP stimuli with subtle flickering adapted to brain-display interactions

2017 J. Neural Eng. 14 016018

(http://iopscience.iop.org/1741-2552/14/1/016018)

OPEN ACCESS
IOP Publishing

Journal of Neural Engineering

J. Neural Eng. **14** (2017) 016018 (15pp)

doi:10.1088/1741-2552/aa550d

Polychromatic SSVEP stimuli with subtle flickering adapted to brain-display interactions

Yu-Yi Chien[1], Fang-Cheng Lin[1,4], John K Zao[2,4], Ching-Chi Chou[1], Yi-Pai Huang[1], Heng-Yuan Kuo[2], Yijun Wang[3], Tzyy-Ping Jung[3] and Han-Ping D Shieh[1]

[1] Department of Photonics, National Chiao Tung University, 30010 Hsinchu, Taiwan
[2] Department of Computer Science and Institute of Biomedical Engineering, National Chiao Tung University, 30010 Hsinchu, Taiwan
[3] Swartz Center for Computational Neuroscience, University of California, San Diego, La Jolla, 92093 CA, USA

E-mail: fclin.eo93g@nctu.edu.tw and jkzao@pet.cs.nctu.edu.tw

Received 6 September 2016, revised 16 December 2016
Accepted for publication 21 December 2016
Published 16 January 2017

Abstract

Objective. Interactive displays armed with natural user interfaces (NUIs) will likely lead the next breakthrough in consumer electronics, and brain-computer interfaces (BCIs) are often regarded as the ultimate NUI-enabling machines to respond to human emotions and mental states. Steady-state visual evoked potentials (SSVEPs) are a commonly used BCI modality due to the ease of detection and high information transfer rates. However, the presence of flickering stimuli may cause user discomfort and can even induce migraines and seizures. With the aim of designing visual stimuli that can be embedded into video images, this study developed a novel approach to induce detectable SSVEPs using a composition of red/green/blue flickering lights. *Approach.* Based on the opponent theory of colour vision, this study used 32 Hz/40 Hz rectangular red-green or red-blue LED light pulses with a 50% duty cycle, balanced/equal luminance and 0°/180° phase shifts as the stimulating light sources and tested their efficacy in producing SSVEP responses with high signal-to-noise ratios (SNRs) while reducing the perceived flickering sensation. *Main results.* The empirical results from ten healthy subjects showed that dual-colour lights flickering at 32 Hz/40 Hz with a 50% duty cycle and 180° phase shift achieved a greater than 90% detection accuracy with little or no flickering sensation. *Significance.* As a first step in developing an embedded SSVEP stimulus in commercial displays, this study provides a foundation for developing a combination of three primary colour flickering backlights with adjustable luminance proportions to create a subtle flickering polychromatic light that can elicit SSVEPs at the basic flickering frequency.

Keywords: brain-computer interface, interactive display systems, steady-state visual evoked potentials, visual stimuli, polychromatic, subtle flickering, canonical correlation analysis

S Supplementary material for this article is available online

(Some figures may appear in colour only in the online journal)

[4] Authors to whom any correspondence should be addressed.

1. Introduction

Eco-friendly three-dimensional (3D) liquid crystal displays (LCDs) with air-touch interactive gesture recognition [1–3] are the latest innovation in *interactive display systems*. These and other novel interactive display technologies started a trend to arm audio-visual systems with natural user interfaces (NUIs). Among these NUIs, wearable brain-computer interfaces, a.k.a. augmented brain-computer interfaces (A-BCIs) [4], promise the ultimate experience in human-machine interaction—one that will enable smart appliances and intelligent environments to respond proactively to a user's cognitive and emotional states [5]. Because vision is the dominant human sensory system, BCI-enabled interactive displays will have a wide range of potential applications in gaming [6], infotainment [7] and e-learning [8]. Figure 1 shows the functional architecture of a brain-display interactive (BDI) system, which is a brain monitoring device integrated with a display/goggle. In such a system, the polychromatic composite lights produced by the liquid crystal or active-matrix organic LED (AMOLED) panels can supply exogenous stimulation to the human visual cortex. Viewers' electroencephalographic (EEG) responses and motor behaviours, such as eye and finger movements, can be analysed to predict their mental states and intentions. These predictions can then be fed back to the interactive display system to adapt the display contents and their presentations.

Among the various BCI modalities [9], steady-state visual evoked potentials (SSVEPs), which can be induced by lights flickering at constant spatial-temporal frequencies and extracted from the EEG signals acquired from the viewer's occipital region [10], may be the most suitable modality to mediate brain-display interactions. In the past decade, SSVEP-based BCI systems have already been used in assisted living [11–13] and gaming [6]. Due to breakthroughs in stimulation modulation and signal processing techniques, SSVEP-BCI has achieved unprecedentedly high information transfer rates [14–16] and was recently developed in an online setting with beamforming [17, 18].

Although SSVEP-BCI has the advantages of being non-intrusive and robust as well as offering high information transfer rates [19], it has a major shortcoming: its flickering stimuli can be distracting, discomforting or even potentially hazardous to viewers. The flickering frequencies used in SSVEP research can be classified into three frequency bands: low (<12 Hz), medium (12–30 Hz) and high (30–60 Hz) frequency subsystems [20]. For the sake of inducing strong SSVEP responses, most SSVEP-BCIs employ visual stimuli in the low- and medium-frequency bands [11, 14, 15, 21–25]. Bright lights (usually in a white colour) flickering in this frequency range are not only distracting to viewers who want to pay attention to the displayed images but can also cause visual fatigue [26], migraine headaches [27] and even photosensitive epilepsy attacks [28–30]. In recent years, there have been substantial efforts to employ high-frequency visual stimuli to induce detectable SSVEP responses [13, 31–33]. Wang and Gao at Tsinghua University [34] and Garcia Molina at Philips Research in Europe [35] are among the pioneers in this area. In the future, if embedded displayed images of less distractive high-frequency stimuli prove feasible, it will allow SSVEPs to be employed more freely among interactive display systems. We have engaged in the design of *high-frequency polychromatic SSVEP stimuli* since 2011 [36–38]. This paper is a report of our preliminary results.

As the first step, this study explored the possibility of using red–green–blue (R/G/B) composite lights flickering at approximately 30–40 Hz as effective stimuli to induce detectable SSVEP responses from the human fovea while reducing the perceived flickering sensation these lights may cause by tuning the flickering frequencies, the relative luminance and the phase shifts among the component lights. Again, pioneers in the field have accomplished a great deal of exploratory work; Cheng and Gao at Tsinghua University performed the first polychromatic SSVEP experiment in 2001 [39], and Bieger and Garcia Molina conducted a series of comprehensive experiments in 2010 to study the effects of various visual stimulation properties, including the flickering frequencies, phases, waveforms, colours, luminance, contrast and patterns, on SSVEP detection accuracy, information transfer rates and user comfort levels [40]. Early attempts also employed polychromatic stimuli in SSVEP-BCI applications [41]. Among the related works, Cheng and Gao's experiment merely demonstrated the feasibility of inducing SSVEP responses using red and green lights flickering at different frequencies. In contrast, Bieger *et al* [42] provided essential information for designing SSVEP stimuli but did not examine the interactions among different stimulus properties, which is an exercise that is crucial for the design of optimal stimuli. Again, none of these works addressed the difficulty of blending the visual stimuli into the displayed images, which is a critical issue in the implementation of a practical brain-display interaction system.

The remainder of this paper expounds our work in five sections. Section 2 explains the rationale underlying the choices of colours, flicker frequencies, relative luminance and phases among the component lights. Section 3 describes the experimental procedures and the analysis techniques employed. Section 4 reports our findings on viewers' flicker perception towards different stimuli and the sideband signal-to-noise ratios (SB-SNRs) of their SSVEP responses. Section 5 discusses the implications of the experimental results along with the preliminary design of a composite white light based on our findings.

2. Rationale

2.1. Underlying principles

The aim of this study was to identify the composition of R/G/B primary colour lights under the proper combination of flickering frequencies, relative luminance and phase shifts that can induce SSVEP responses with the highest SB-SNRs from viewers' occipital lobes while reducing the perception of flickering sensations. We based the design of our experiments on the following supporting evidence.

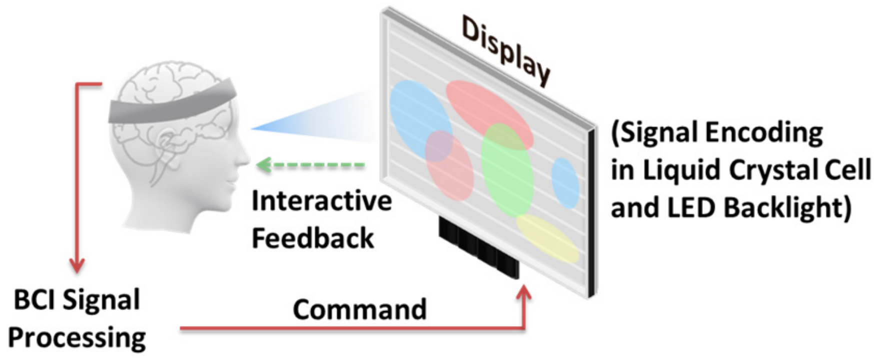

Figure 1. Functional block diagram of a brain-display interaction (BDI) system.

Lin *et al* [36] showed that SSVEPs induced by *foveal stimulation* spanning a 2° view angle with white LED lights flickering between 25 Hz and 45 Hz exhibit enhanced SB-SNRs that were compatible with those evoked by similar stimuli in the EEG alpha band. Furthermore, our experiments with primary colour stimuli detected similar SB-SNR increases among foveal SSVEP responses towards red- and green-coloured lights [43]. In both cases, viewers' flicker perceptions of the stimuli decreased as the flickering frequencies of the stimuli increased.

A plausible explanation of these results is that although the power of both the SSVEP responses and the ambient EEG signals diminished at higher frequencies, their power ratios at neighbouring frequencies may not diminish with the rise in frequency [34]. Foveal SSVEP responses towards polychromatic lights may be strong due to the high concentration of cone photoreceptors in the human fovea. In contrast, the diminishing (and even vanishing) of viewers' flickering sensation at higher frequencies may be explained by the presence of critical flicker frequency (CFF) thresholds of the cone photoreceptors within that frequency range. The SB-SNRs hinted at the possibility of the robust detection of foveal SSVEP responses at those frequencies while increasing viewer comfort by diminishing the perceived flickering sensation.

The second type of supporting evidence came from the experimental findings of Shady *et al* [44] and Jiang *et al* [45]. Both teams observed that when equal luminous red and green lights flickered alternatingly at frequencies of 25 Hz or above, the two primary lights could fuse into a non-flickering composite yellow light. Using functional magnetic resonance imaging (fMRI), Jiang *et al* [45] also showed that the composite yellow light activated different visual cortical areas than those activated by a non-flickering mono-chromatic yellow light. Their findings suggested that reducing the flickering sensation of the visual stimuli is possible with the use of composite lights. The fMRI results further hinted that primary colour lights can induce SSVEP responses; however, they appeared fused in colour to the viewers.

Finally, we based our colour composition on Hering's *opponent-process theory of colour vision* [46]. Among the R/G/B primary colours, this study chose dual red–green (R/G) and red–blue (R/B) composite lights as the stimulating light sources in the experiments. These choices made the experiments compatible with those conducted by Jiang *et al* [45] and Bieger *et al* [42].

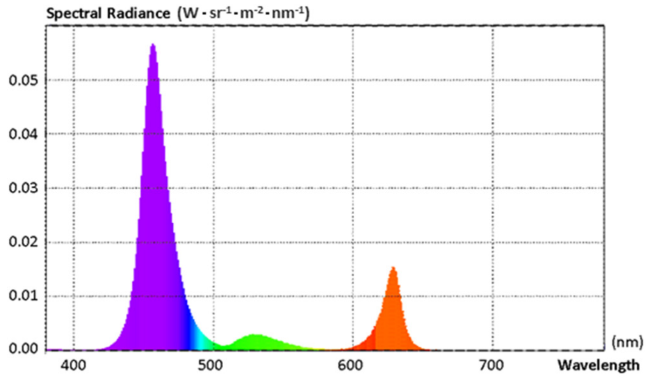

Figure 2. Spectral radiance of commercially available LED lights in red (620–645 nm), green (520–550 nm) and blue (460–490 nm) colours.

According to the opponent-process theory, colour perception is formed by *antagonistic interactions* (excitation ± versus inhibition −) among the ganglion cells connected to the cone photoreceptors. The antagonism forms two opponent colour channels known as (R+G −) and (B+Y −). The ratio between the responses of these channels produces the sensation of the hue, whereas the combination of their responses produces the sensation of *colourfulness*. The following description shows the neural circuit schematics of these two opponent colour channels: in the (R+G −) channel, the primary red and green colours interact antagonistically, whereas in the (B+Y −) channel, the yellow colour is first formed by combining red and green excitation as Y= (R+G +) [47]. Then, the composite yellow colour interacts antagonistically with the primary blue colour. According to this theory, the interaction between the red and green colours belongs to the R–G opponent colour channel, whereas the interaction between the red and blue colours does not belong to any opponent colour channel. The choices of the two colour pairs thus enabled us to compare the responses of these two conditions.

2.2. Pragmatic design of composite stimuli

In planning the experiments, some design decisions were made to improve the commercial value of our findings. First, we decided to use commercially available red/green/blue LEDs as the primary light sources. The Spectral radiance of the commercially available LED lights is shown in figure 2.

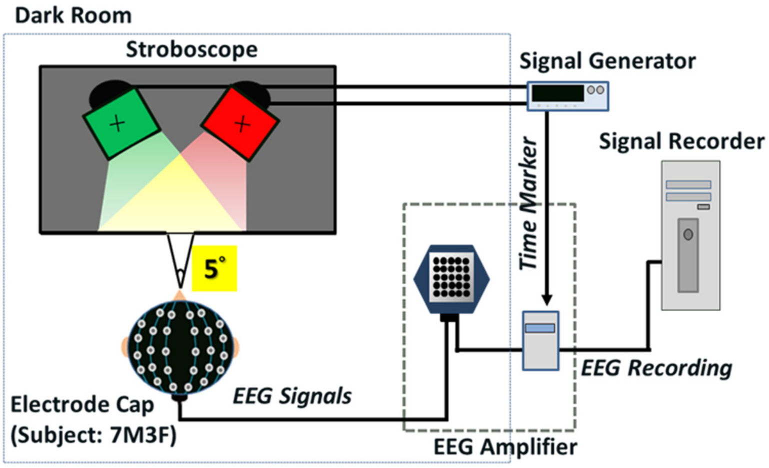

Figure 3. Block diagram of the SSVEP experimental setup with the red and green (R/G) composite coloured lights.

The light sources are widely used in LCDs with LED backlights [48] and in organic LED (OLED) and future quantum dot LED (QD-LED) displays [49]. As an additional virtue, the narrow colour spectra of these light sources enable them to selectively stimulate long (L), medium (M) and short (S) wavelength cone photoreceptors.

We also employed rectangular waveforms with a 50% duty cycle for all component lights because Teng *et al* [50] observed that such waveforms were more effective in inducing SSVEP responses than sinusoidal waveforms or triangular waveforms with higher or lower duty cycles. These symmetrical rectangular waveforms are also more similar to the actual waveforms generated by the LCD and OLED displays.

Finally, we adopted the concepts of balanced and equal luminance in the design of the composite stimuli. The term *balanced luminance* indicates that the proportions of luminance of the two component lights, R/G or R/B, permit the formation of white light through the addition of an appropriate proportion of the third primary colour light. Because the relative luminance of the R/G/B components requires a ratio of 3:6:1 in a composite white light [51], the balanced luminance ratios of the R/G and R/B components were 2 : 1 and 3 : 1, respectively. We adopted balanced luminance solely to produce a white composite light by adding a third compensating component.

As an alternative, this study also applied *equal luminance* to the two component lights, R/G or R/B, which means that the luminance ratios remained 1 : 1 regardless of the choice of colours. Because the component lights are equal in luminance, the composite lights resulting from alternatingly flickering these components were expected to produce the weakest flickering sensation. This study compared the flickering sensation induced by these two different luminance profiles.

3. Methods

To observe both the SB-SNRs of the foveal SSVEP responses and the subjective flickering sensations towards the two composite colour lights at different flickering frequencies, relative luminance and phase shifts, two separate experiments with the same groups of subjects were conducted on different days: the first experiment was performed with the red–green (R/G) composite lights, whereas the second included the red–blue (R/B) composite lights.

Table 1. Combinations of the control variable values (Supplementary material available from stacks.iop.org/JNE/14/016018/mmedia).

Component colours	Frequency (Hz)		Luminance (cd m^{-2})		Relative phase (°)
Red and green (R/G)	{32, 40}	×	{R: 76.5, G: 76.5; R: 51, G: 102}	×	{0, 180}
Red and blue (R/B)	{32, 40}	×	{R: 76.5, G: 76.5; R: 114.75, G: 38.25}	×	{0, 180}

3.1. Subjects

Ten healthy subjects (seven males and three females), aged between 20 and 25 years (mean 22.3 years; SD 1.8), participated in the two aforementioned experiments. All subjects had normal or corrected-to-normal visual acuity without vision impairment. They also had no neurological abnormalities and were clearly informed that flickering stimulation might induce epileptic seizures. Informed consent was obtained before each subject's participation. The subjects' consent form was approved by the Research Ethics Committee for Human Subject Protection at National Chiao Tung University (application number: NCTU-REC-102-008).

3.2. Apparatus

To prevent potential contamination of the visual stimuli and the EEG signals by ambient light and electromagnetic radiation, the experiments were conducted in a darkened, shielded recording chamber. Figure 3 illustrates the apparatus used in the experiments. The R/G and R/B composite colour stimuli were produced by two LED-powered stroboscopes (MVS 115/230, Monarch, Amherst, NH, USA) driven by a dual-channel waveform generator (33522A, Agilent, Santa Clara, CA, USA) to generate signal waveforms with precise amplitudes, frequencies and relative phase offsets. The composite

Table 2. Chromaticity coordinates of the primary colour and R/G and R/B composite lights.

xy coordinates	Primary colours	R/B composite lights		R/G composite lights	
		Balanced lumin.	Equal lumin.	Balanced lumin.	Equal lumin.
Blue	(0.145, 0.038)	(0.298, 0.116)	(0.207, 0.069)		
Red	(0.690, 0.309)				
Green	(0.230, 0.718)			(0.476, 0.499)	(0.553, 0.431)

lights were projected onto a viewing screen erected 50 cm in front of the subject and passed through a 4.4 cm circular translucent area spanning a 5° viewing angle.

The EEG data were obtained using a non-invasive 64-channel Quik-Cap, which placed the electrodes on the subject's scalp according to the international 10–20 system, and were recorded using an EEG amplifier (SynAmps^2 model 8050, Neuroscan, El Paso, TX, USA) and a desktop computer. Furthermore, a transistor–transistor logic-synchronization (TTL-SYNC) signal was fed from the waveform generator into the EEG recording system to supply the 'time ticks' marking the firing of the stimulating light pulses.

3.3. Control parameters

In the experiment, binary choices were made among the values of the four parameters controlling each component light: (1) component colours, (2) flickering frequency, (3) luminance, and (4) relative phase. Table 1 lists the combinations of values adopted in the different rounds of the experiments.

In terms of the *flickering frequency*, 32 Hz and 40 Hz were used as the two samples from the range of 25–45 Hz based on Lin *et al* [36]. These choices, 32 Hz and 40 Hz, belong to the high-frequency range (30–60 Hz) according to Regan [20] and were employed with the aim of studying the effects of diminished EEG responses on the SB-SNRs of the SSVEP responses.

In terms of the *relative phase* between the flickering component lights, the choice was between 0° and 180°. A phase shift of 0° implies a complete overlap of the two flickering lights; the two component lights turn ON and OFF simultaneously with their pulses superimposed onto each other. Thus, the composite light appears to have bright light pulses interlaced with dark intervals. In contrast, a phase shift of 180° implies an alternating flicker of the two component lights; the pulses of the component lights interlace with each other, thus amortizing the brightness of their pulses and eliminating the dark intervals from their composite light.

Finally, in terms of *luminance*, a reasonable level for the total luminance was set and then divided proportionally among the component lights. To determine the balanced luminance of the R/G component lights, white light at 170 cd m^{-2}, which is the typical luminance of the white background appearing on an LCD monitor during daytime, was divided into a ratio of 3 : 6 : 1. Hence, the red light was set at 51 cd m^{-2} and the green light was set at 102 cd m^{-2}, and the lights contributed a total of 153 cd m^{-2}, which is 90% of 170 cd m^{-2}; the remaining 10% (17 cd m^{-2}) was reserved for the luminance of the compensating blue light.

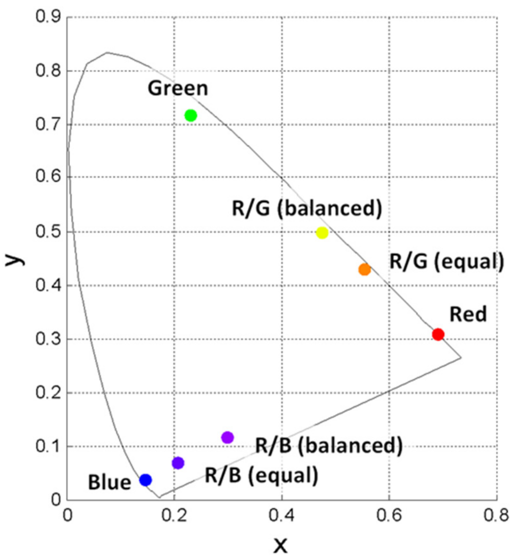

Figure 4. The *xy* coordinates of the composite stimuli in a CIE 1931 chromaticity diagram.

To expose the subjects to visual stimuli at the same luminance level, we set the total luminance of the dual-colour stimuli at 153 cd m^{-2} throughout the experiments and divided it into proper proportions. In the case of equal luminance, the luminance of each component light was set at 76.5 cd m^{-2} regardless of its colour. In the case of balanced luminance between the R/B lights, we set the luminance at a 3 : 1 ratio, such that the red light was at 114.75 cd m^{-2} and the blue light was at 38.25 cd m^{-2}.

The net effect of varying the luminance ratios between the component lights was to change the apparent colour of the composite lights, which was often specified in terms of the chromaticity *xy* coordinates in the International Commission on Illumination (CIE) 1931 colour space [52]. Table 2 and figure 4 provide the chromaticity coordinates of the R/G/B primary colours and the composite colours with balanced and equal luminance.

3.4. Procedures

During the experiments, each subject was asked to sit in a chair, place his/her head on a chin-rest and stare at the centre of the 5° diffused light source. Visual stimulations in the form of composite lights with different flicker frequencies, luminances and relative phases were presented to the subject in rounds, each of which lasted 50 s with a 30 s rest period between each stimulation. To eliminate potential interference between adjacent rounds, each subject underwent the experimental rounds in a randomized order.

Table 3. Specification of the standardized (five-point) subjective flicker perception scores.

1	2	3	4	5
Imperceptible	Perceptible but not annoying	Slightly annoying	Annoying	Very annoying

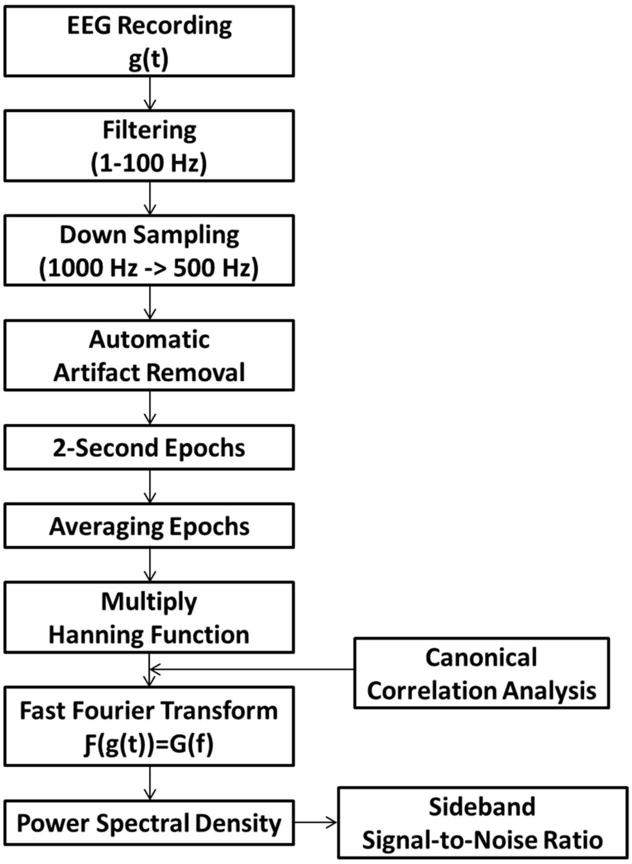

Figure 5. SSVEP signal analysis flow chart.

In each experimental round, the EEG signals from 64 channels were sampled at 1000 Hz and recorded along with the TTL-SYNC signal from the waveform generator. Furthermore, the subjects also graded the flicker perception of the stimuli based on a standardized five-point scale for the subjective assessment of television picture quality [53], with *one* indicating imperceptible flickering and *five* implying very annoying flickering (table 3). We chose a subjective flickering score of *two* as the tolerable flickering threshold of the visual stimuli.

3.5. Data processing

The signal analysis procedures, which comprised signal pre-processing, segmentation and epoch averaging, are depicted in figure 5. Both the EEG signals captured from each subject and their ensemble averages were analysed to discover the general trends and individual differences. First, to decrease the data size while maintaining the accuracy of the high-frequency data, the EEG signal was filtered (1–100 Hz), and the sampling rate was lowered (500 Hz). Then, automatic artefact removal, including independent component analysis (ICA)-based algorithms [54, 55], was used to ensure that the data contained no events with abnormally strong power and to remove blinks, eye movements and discontinuities from the data while leaving brain activity almost unaffected. Next, this study divided the 50 s EEG signal into 25 two-second epochs to increase the strength of the signal while obscuring noises using epoch synchronized averaging. The Hanning function, which is represented in equation (1), was utilized to minimize the effect of spectral leakage [56]:

$$w(n) = 0.5\left(1 - \cos\left(2\pi\frac{n}{N-1}\right)\right), \quad 0 \leqslant n \leqslant N-1 \qquad (1)$$

where $N = 1000$ is the number of sample points.

The SSVEP signals of each subject extracted from the nine parietal and occipital channels, namely P1, PZ, P2, PO3, POZ, PO4, O1, OZ and O2, were analysed. The single-channel method analysed only the EEG signal extracted from the Oz channel, whereas the multi-channel method processed the signals from all nine channels using the canonical correlation analysis (CCA) technique [57]. This technique computes the maximum correlation between a linear combination of multi-channel EEG signals X and a combination of the reference sinusoidal signals Y_f:

$$Y_f = \begin{bmatrix} \sin\left(\frac{2\pi nf}{f_s}\right) \\ \cos\left(\frac{2\pi nf}{f_s}\right) \end{bmatrix} \text{with } n = 1 \ldots N \qquad (2)$$

where f is the target frequency and f_s is the sampling rate. Considering two multidimensional variables (EEG signals X and the reference signals Y), the CCA method finds the weight vectors $(\boldsymbol{w}_x, \boldsymbol{w}_y)$ that maximize the correlation between their linear combinations (x, y). This method can be used to find the linear combination of multi-channel EEG signals with maximum correlation ρ with the reference signals [22]:

$$\max_{w_x, w_y} \rho(x, y) = \frac{E\,[\mathbf{w}_x^T XY^T \mathbf{w}_y]}{\sqrt{E\,[\mathbf{w}_x^T XX^T \mathbf{w}_x]\,E\,[\mathbf{w}_y^T YY^T \mathbf{w}_y]}} \qquad (3)$$

Then, the single-channel signals from Oz and the spatially weighted multi-channel signals (x) using CCA were analysed using fast Fourier transform (FFT) with Hanning windows. Their power spectral density (PSD) was computed using equation (4):

$$\text{PSD}(f) = \frac{N}{f_s}\,|G(f)|^2 \qquad (4)$$

where $|G(f)|$ is the Fourier amplitude of the signal at the frequency f and N/f_s is the epoch length. The sideband SNR (SB-SNR) was defined as the ratio between the signal power and the sideband noise power at the decibel (dB) scale as represented in equation (5) [34]:

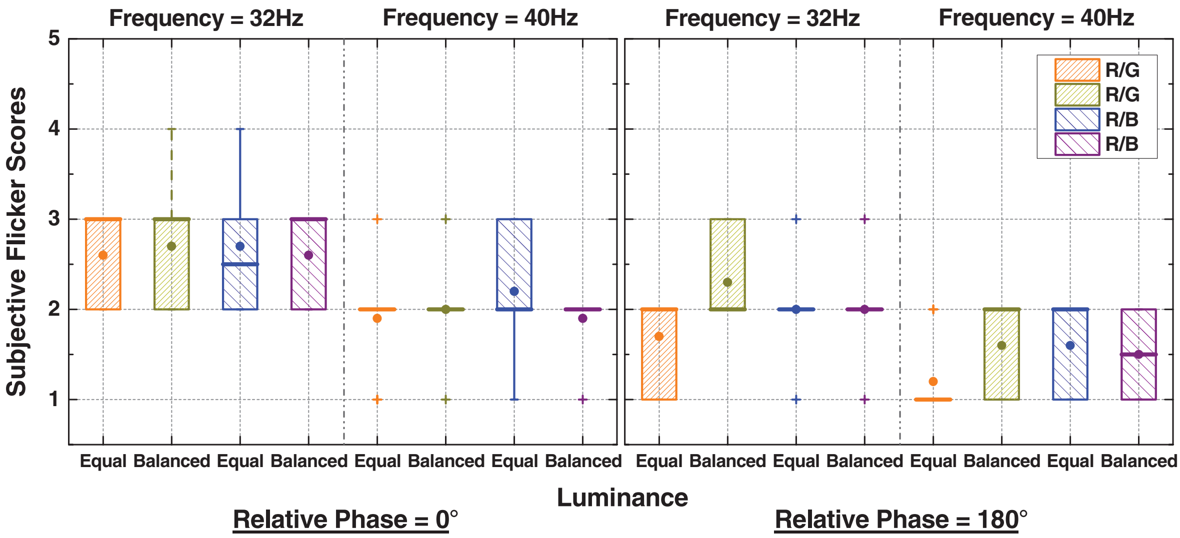

Figure 6. Subjects' foveal flicker perceptions for the composite R/G lights and R/B lights with a 50% duty cycle at 32 Hz/40 Hz flickering frequencies, equal/balanced luminance and 0°/180° relative phases. The boxes in the figure cover the mid-50% of the scores, the thick horizontal bars indicate the median values, and the solid dots and crosses indicate their average values and the outliers, respectively.

Table 4. Four-way rANOVA results for the subjective flicker perception scores.

	Phase (P)	Frequency (F)	Colour (C)	Luminance (L)		
F value[a]	23.640	26.125	0.849	1.830		
p value[b]	0.001**	0.001**	0.381	0.209		
	$P \times F$	$P \times C$	$P \times L$	$F \times C$	$F \times L$	$C \times L$
F value[a]	0.849	0.036	5.211	0.584	1.552	8.103
p value[b]	0.381	0.853	0.048*	0.464	0.244	0.019*
	$P \times F \times C$	$P \times C \times L$	$P \times F \times L$	$F \times C \times L$		
F value[a]	0.043	1.000	0.184	0.053		
p value[b]	0.840	0.343	0.678	0.823		
	$P \times F \times C \times L$					
F value[a]	0.669					
p value[b]	0.434					

[a] Degrees of freedom = (1, 9) for each rANOVA on the different factors.
[b] Superscript *, ** and *** denote $p < 0.05$, $p < 0.01$ and $p < 0.001$, respectively.

$$\text{SB-SNR}(f) = \frac{\text{PSD}(f)}{\frac{1}{n-2}\sum_{k=2}^{n/2}[\text{PSD}(f+k\Delta f) + \text{PSD}(f-k\Delta f)]} \tag{5}$$

where $\Delta f = f_s/N = 0.5$ Hz is the frequency resolution and $n = 8$ was used in the calculation. Leakage was the main reason we avoided the adjacent ± 1 unit ($k = 2$) sideband noise power from our stimulus frequencies.

3.6. Statistical analyses

This study involved four parameters, as mentioned in section 3.3. Therefore, a four-way repeated-measures analysis of variance (rANOVA) [58, 59] was conducted using SPSS software (SPSS Statistics 17.0, IBM Corporation, Endicott, NY, USA) to examine the null hypothesis, i.e. the different flickering frequencies/relative phases/luminance/colours would not affect the SSVEP responses and flicker perception. The rANOVA analysed the main effects of and interactions among the independent variables on the experimental outcomes, with significance set at 0.05. The Greenhouse–Geisser correction was applied if the data did not conform to the sphericity assumption based on Mauchly's test of sphericity. All *post hoc* pairwise comparisons were corrected using the Bonferroni's test.

4. Results

With the aim of identifying the optimal composite colour stimuli that can induce the strongest foveal SSVEP responses while causing negligible flicker perception, this study examined the *flicker perception* of ten healthy subjects and the *SB-SNR* of their foveal SSVEP responses towards the composition of R/G and R/B dual-colour lights flickering at different frequencies, relative luminances and phase offsets (section 3.3). An rANOVA was used to identify the statistically significant differences among the SSVEP responses towards the different compositions. The optimal composition was selected as the

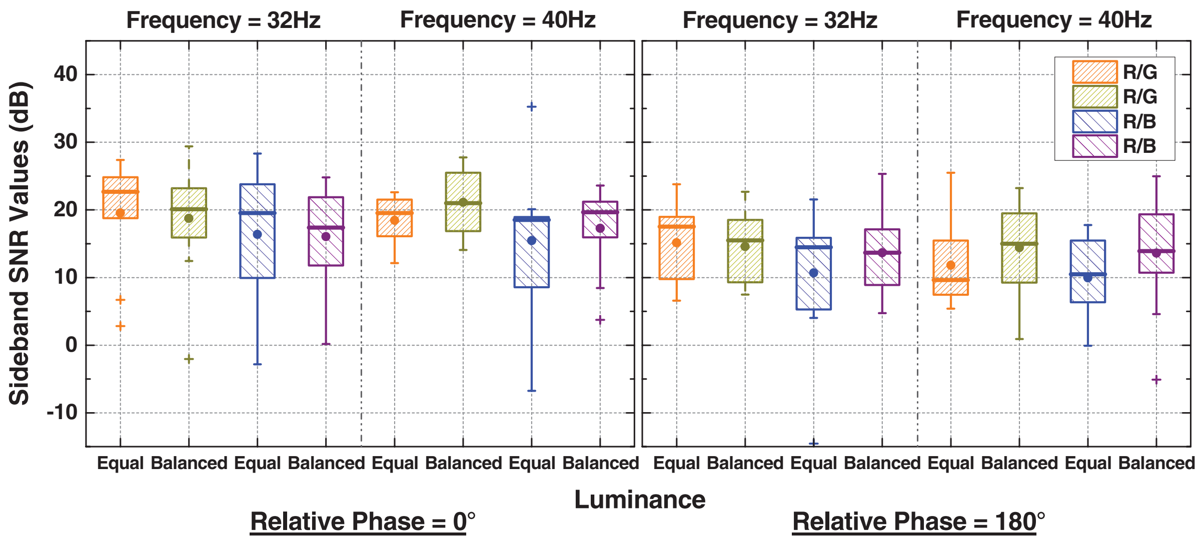

Figure 7. Boxplots of the sideband SNR (dB) values of the SSVEP signals collected at the Oz channel in response to the composite R/G lights and R/B lights. The boxes in the figure cover the mid-50% of the scores, the thick horizontal bars indicate the median values, and the solid dots and crosses indicate their average values and the outliers, respectively.

one that induced SSVEP responses with significantly higher SNR values while maintaining a subjective flickering perception lower than two in the standard five-point scale (section 3.4). The efficacy of these composite stimuli was then verified by analysing their accuracy in detecting the SSVEP frequencies using the CCA method.

4.1. Flicker perception

We aimed to discriminate the different composite stimuli with respect to subjects' flickering perceptions of these stimuli. Only those stimuli with average flickering scores of less than two (of five), indicating that flickering was perceptible but *not* annoying, were selected for further consideration. We also attempted to identify the factors (among colour, frequency, phase and luminance) with the most significant effects on the subjective flickering sensation.

Figure 6 shows a boxplot of the standardized five-point flicker subjective perception scores given by the ten subjects towards the composite R/G and R/B lights with a 50% duty cycle at different flickering frequencies, luminances and relative phases. Table 4 presents the rANOVA results for flicker perception.

The following observations were made based on the subjective perception scores:

1. The composite lights with 180° phase offsets (or alternating pulsation) always produced lower flicker perception scores than the lights with 0° offset (or perfectly aligned pulses). Among the four-way rANOVA results, the main effect of relative phase was significant ($F[1, 9] = 23.640$, $p = 0.001$).
2. The flicker perception scores given to the composite R/G and R/B stimulations were approximately compatible with the scores given to the stimulation with the white LED light in a similar SSVEP experiment reported in [37]. In both cases, the stimuli at 40 Hz appeared to be less flickering than those at 32 Hz. Among the four-way rANOVA results, the main effect of frequency was significant ($F[1, 9] = 26.125$, $p = 0.001$).

Table 4 also shows that the interaction between phase and luminance ($F[1, 9] = 5.211$, $p = 0.048$) and the interaction between colour and luminance ($F[1, 9] = 8.103$, $p = 0.019$) were significant.

The significant interaction between phase and luminance indicated that in the 180° condition, the balanced luminance group had more flickering than the equal luminance group ($\mu = 1.850$ versus $\mu = 1.625$), whereas in the 0° condition, the balanced luminance group was approximately identical to the equal luminance group ($\mu = 2.300$ versus $\mu = 2.350$). The difference between the balanced luminance and equal luminance groups in the 180° condition was significant ($p = 0.011$), whereas the difference in the 0° condition was not significant ($p = 0.570$).

The significant interaction between colour and luminance indicated that, in the equal luminance condition, the R/B group was more flickering than the R/G group ($\mu = 2.125$ versus $\mu = 1.850$), whereas in the balanced luminance condition, the R/B group was approximately identical to the R/G group ($\mu = 2.000$ versus $\mu = 2.150$). The difference in the equal luminance condition between the R/G and R/B groups was significant ($p = 0.010$), whereas the difference in the balanced luminance condition was marginally significant ($p = 0.057$).

4.2. Sideband signal-to-noise ratios (SB-SNRs)

The accurate detection of SSVEP responses depends greatly on the SNRs between the power of the SSVEP signals versus the power of the ambient signals at the stimulation frequencies. This section examines the SB-SNRs of the foveal SSVEP responses with the aim of identifying the optimal stimuli.

Boxplots of the SSVEP SB-SNR (dB) values using the single-channel method and the multi-channel method are

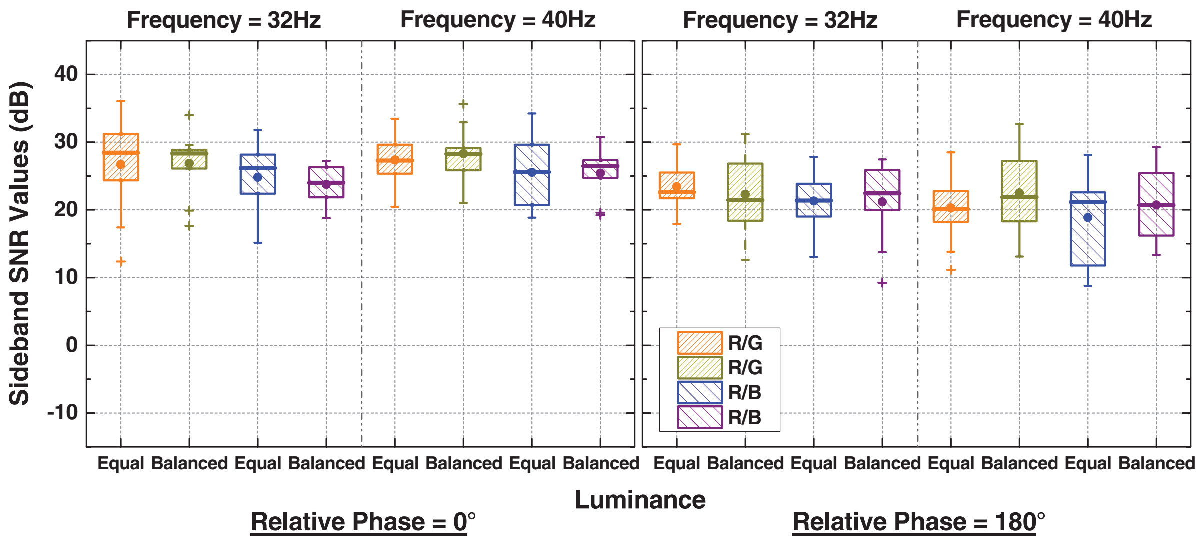

Figure 8. Boxplots of the sideband SNR (dB) values of the CCA-combined multi-channel SSVEP signals in response to the composite R/G lights and R/B lights. The boxes in the figure cover the mid-50% of the scores, the thick horizontal bars indicate the median values, and the solid dots and crosses indicate their average values and the outliers, respectively.

Table 5. Four-way rANOVA results for the SSVEP SB-SNR values using the CCA method.

	Phase (P)	Frequency (F)	Colour (C)	Luminance (L)		
F value[a]	49.327	0.039	2.385	0.274		
p value[b]	0.000***	0.848	0.157	0.613		
	$P \times F$	$P \times C$	$P \times L$	$F \times C$	$F \times L$	$C \times L$
F value[a]	7.248	0.259	0.356	0.008	3.032	0.078
p value[b]	0.025*	0.623	0.566	0.932	0.116	0.786
	$P \times F \times C$	$P \times C \times L$	$P \times F \times L$	$F \times C \times L$		
F value[a]	0.004	0.178	0.443	0.110		
p value[b]	0.950	0.683	0.522	0.747		
	$P \times F \times C \times L$					
F value[a]	0.150					
p value[b]	0.707					

[a] Degrees of freedom = (1, 9) for each rANOVA on the different factors.
[b] Superscript *, ** and *** denote $p < 0.05$, $p < 0.01$ and $p < 0.001$, respectively.

shown in figures 7 and 8, respectively. The data in figure 7 were collected at the Oz channel in response to the composite R/G or R/B lights. The results indicate that both the R/G and R/B composite coloured lights evoked distinct SSVEPs. The individual differences affected the SNR distribution, as shown in the boxplots. The SB-SNR (dB) values of the SSVEPs extracted using the single-channel (Oz) method showed variations.

Recently, a multi-channel method using CCA has been widely used to improve classification accuracy in SSVEP-based BCIs [14, 22, 60–63]. The SB-SNRs in figure 8 were calculated from the canonical variables for the recorded EEG data. The spread of the SB-SNRs extracted from the multi-channels was narrower than that extracted from the Oz channel. In addition, the average SSVEP SNR values were 8.3 dB higher than those extracted using the single-channel method. These results support CCA as a more robust technique for quantifying SSVEP responses.

To assess the significant differences, this study applied a rANOVA to compare the SB-SNR (dB) values of the SSVEPs using the CCA method towards composite stimuli with different combinations of colours, flickering frequencies, phase shifts and luminance levels (table 5).

The following observations were made based on the SSVEP SNR values:

1. The average SSVEP response at the fundamental frequency of the 0° relative phase was larger than that at the fundamental frequency of the 180° relative phase. Among the four-way rANOVA results, the main effect of relative phase was significant ($F[1, 9] = 49.327$, $p < 0.001$).
2. Although there was a significant difference in flicker perception of the composite visual stimuli with the different flickering frequencies, the SSVEP SNR values of the stimuli at 40 Hz appeared to be similar to those at 32 Hz. Among the four-way rANOVA results, there was no significant effect of frequency ($F[1, 9] = 0.039$, $p = 0.848$).

Table 5 also shows that the interaction between phase and frequency ($F[1, 9] = 7.248$, $p = 0.025$) was significant. The results indicated that in the 180° condition, the SB-SNR

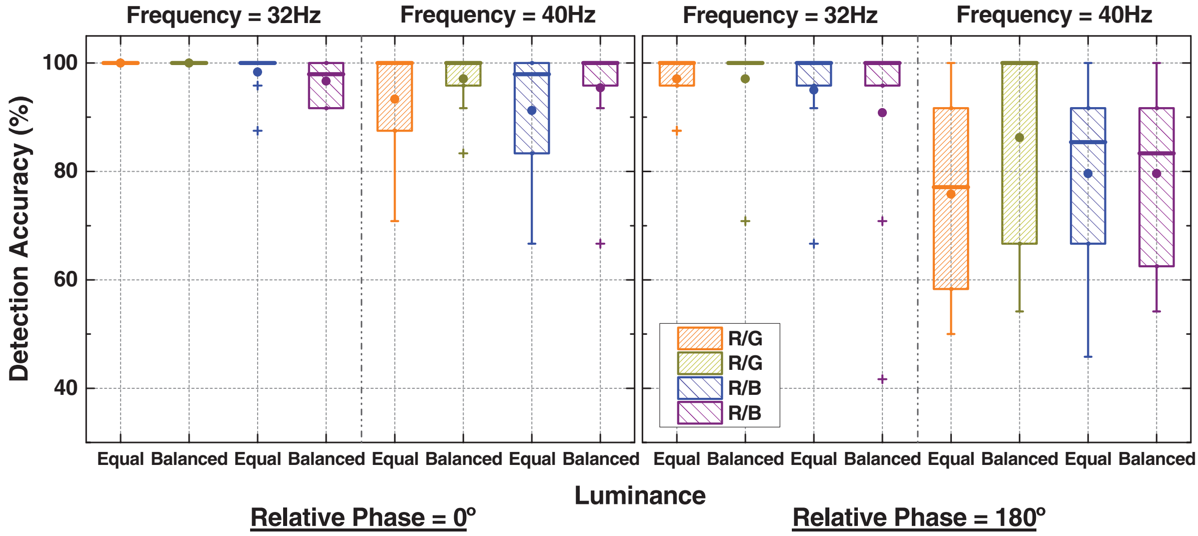

Figure 9. Boxplots of the simulated online classification detection accuracy of the CCA-combined multi-channel SSVEP signals in response to the composite R/G lights and R/B lights. The boxes in the figure cover the mid-50% of the scores, the thick horizontal bars indicate the median values, and the solid dots and crosses indicate their average values and the outliers, respectively.

values of the 32 Hz group were slightly higher than those of the 40 Hz group ($\mu = 22.049$ versus $\mu = 20.593$), whereas in the 0° condition, the SB-SNR values of the 32 Hz group were approximately identical to those of the 40 Hz group ($\mu = 25.544$ versus $\mu = 26.660$). The difference in the 180° condition between the 32 Hz and 40 Hz groups was marginally significant ($p = 0.074$), whereas the difference in the 0° condition was not significant ($p = 0.170$). These results reveal a high correlation between the SB-SNR values and the relative phase/frequency; however, the main effects of colour and luminance were not significant.

4.3. Accuracy of the SSVEP frequency detection

Finally, we compared the statistically significant differences in the SSVEP SB-SNRs with the *accuracy* in detecting the flickering frequencies of the composite stimuli based on the SSVEP fundamental frequencies. Our aims were as follows: (1) to verify the *usability* of the composite stimuli that yielded the high SNR values and (2) to examine the performance of the coherent detection techniques, such as CCA, in discriminating the SSVEP responses.

We performed a simulated online analysis because the composite stimuli were not presented to the subjects simultaneously. Our visual stimuli only showed one target at a time and lasted 50 s in each trial. However, to emulate an online detection process, each two-second epoch of SSVEP signals was passed through the CCA 32 Hz/40 Hz classifier without performing the synchronized averaging step applied in the SB-SNR calculation. We used CCA to discriminate the two fundamental frequencies (32 Hz versus 40 Hz) by comparing the correlation between the SSVEP responses of 25 two-second epochs and the reference sinusoidal signals at these two frequencies. Following the approach of Bin *et al* [22], we selected the frequency of the reference signal that yielded a higher correlation with the SSVEP signal as the classified frequency.

Figure 9 shows the boxplots of the percentages of accurately detected flickering frequencies among the different composite stimuli.

From the boxplots, the following observations are consistent with the SSVEP SB-SNRs mentioned in the previous section.

1. When comparing the different phase offsets, the detection accuracy spread of the alternating pulsation stimulation (180° phase offsets) was much wider ($F[1, 9] = 41.817$, $p < 0.001$).
2. Regarding the different flickering frequencies, the detection of the 32 Hz stimuli was more accurate than the 40 Hz stimuli, with higher median and average accuracies and a narrower value spread ($F[1, 9] = 52.319$, $p < 0.001$).

The results showed that in the 180° condition, the detection accuracy of the 32 Hz group was higher and the spread was narrower than that of the 40 Hz group ($\mu = 95.000$ versus $\mu = 80.313$), whereas in the 0° condition, the SB-SNR values of the 32 Hz group were similar to those of the 40 Hz group ($\mu = 98.750$ versus $\mu = 94.271$). The results also showed that the detection accuracy of the stimuli with a 180° phase shift was lower than that of the stimuli with a 0° phase shift, particularly for the lights that flickered at a higher frequency (40 Hz). The rANOVA results were also consistent with those of the flicker perception and SB-SNR responses. We observed that the flickering frequencies and relative phases were the major factors affecting the accuracy of the frequency detection.

4.5. Correlations

After the analysis of the examination, as shown in the previous sections, we analysed the correlations between the average results of the human behavioural and SSVEP responses (figure 10) and the average results from the SSVEP responses (SB-SNR (dB) values and detection accuracy) (figure 11). Based on these results, we verified the relationship

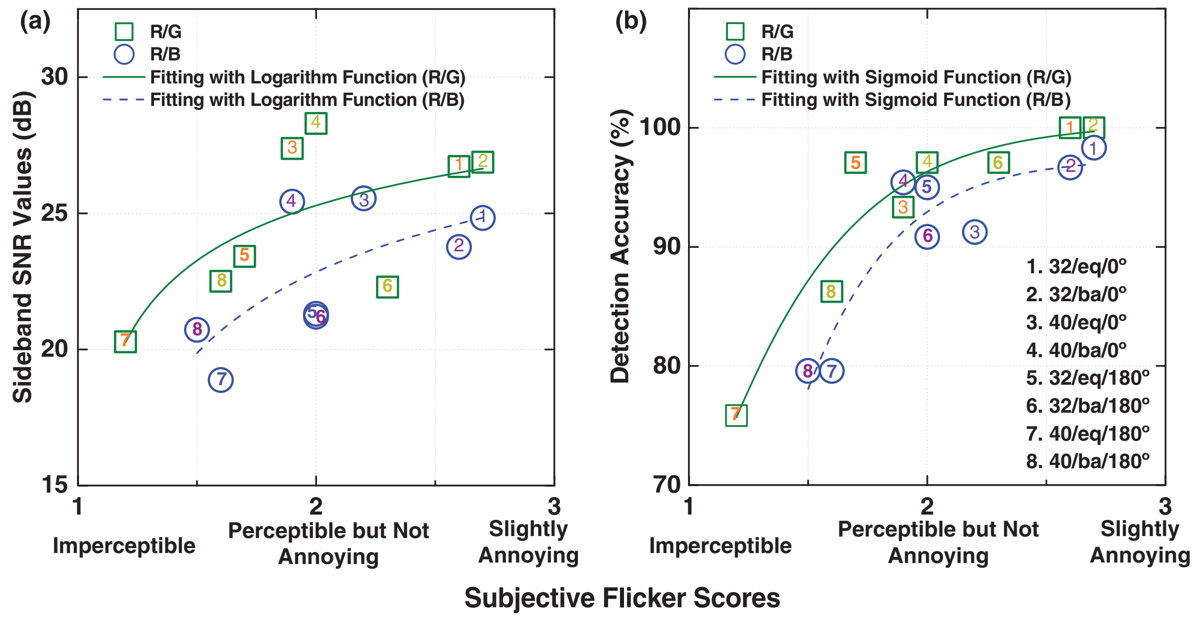

Figure 10. Correlations between the subjects' behaviour and SSVEP responses with the best curve fitting. (a) The fitting of the subjects' average flicker perceptions versus the average sideband SNR (dB) values of the SSVEP signals. (b) The fitting of the subjects' average flicker perceptions versus the average detection accuracies. The boxes in the figure cover the mid-50% of the scores, the thick horizontal bars indicate the median values, and the solid dots and crosses indicate their average values and the outliers, respectively.

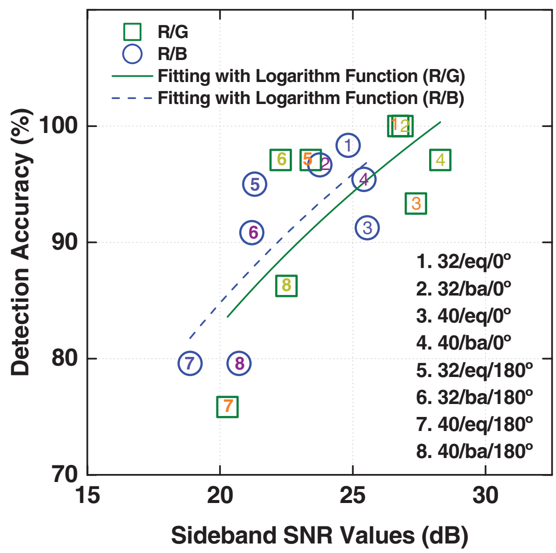

Figure 11. Correlations among the subjects' average sideband SNR (dB) values of the SSVEP signals and the average detection accuracies. The boxes in the figure cover the mid-50% of the scores, the thick horizontal bars indicate the median values, and the solid dots and crosses indicate their average values and the outliers, respectively.

between these responses and determined the suitable visual stimuli for this study. We used a double logarithmic reciprocal function (Bradley) and a sigmoidal logistic function, type 1 (SLogistic1), as shown in figure 10. A two-parameter logarithm function (Log2P1), shown in figure 11, was used to fit the curves using OriginLab software (OriginPro 2015, OriginLab Corporation, Northampton, MA, USA). The Spearman's rank-order correlation for the nonparametric measures was used to determine the relationship [64].

Based on the fitting plot of the subjects' behaviour and SSVEP responses, we made the following observations ((a) and (b) represent the descriptions in figures 10(a) and (b), respectively):

1. (a) The subjects' flicker perceptions and the SB-SNR (dB) values of the SSVEP signals were positively correlated, and the correlation was statistically significant ($r = 0.553$, $p = 0.026$). (b) There was a strong positive correlation between the subjects' flicker perceptions and the detection accuracies, which was statistically significant ($r = 0.819$, $p < 0.001$). The increases in the flicker sensations were correlated with the increases in the SSVEP responses.
2. (a) The settings (180°) caused the least flickering sensation, but the SSVEP SNR values were lower. (b) The settings (40 Hz; 180°) caused the least flickering sensation, but the detection accuracies were lower. In contrast, the settings (32 Hz; 0°) caused stronger flickering sensations, but the detection accuracies were higher.
3. The R/G stimuli outperformed the corresponding R/B stimuli by yielding higher average SB-SNR values and average detection accuracies in all cases. In particular, the R/G stimuli yielded better overall detection accuracies.
4. The R/G stimuli had lower subjective flicker scores, particularly in the equal-luminous condition (please see the explanation in section 5.1).
5. (a) The arithmetic means of the SNR (dB) values were more scattered with respect to the flicker perceptions, particularly when the flicker score = 2 (perceptible but not annoying). Note that the arithmetic means in the dB scale are equivalent to the geometric means in the linear scale. (b) The detection accuracy of both the R/G and R/B stimuli exhibited a sigmoidal trend and approached

100% when the flicker perception > 2.5. The sigmoidal trends of the detection accuracy for both the R/G and R/B stimuli had their inflection points when the flicker perception > 2.

The following stimuli yielded detection accuracy $> 90\%$ with flicker scores $\leqslant 2$ in descending order of flicker scores and then detection accuracies:

R/G Stimuli: [4] 40 Hz/ba/0°, [3] 40 Hz/eq/0°, [5] 32 Hz/eq/180°;

R/B Stimuli: (5) 32 Hz/eq/180°, (6) 32 Hz/ba/180°, (4) 40 Hz/ba/0°.

With the aim of designing visual stimuli that can be embedded into video images, the compositions (detection accuracy $> 90\%$; flicker score $\leqslant 2$) were suitable visual stimuli that induced distinct SSVEP responses and produced the least flicker sensations. In addition, we compared the relationship between the SB-SNR values, which is a crucial signal quality measurement, and the detection accuracies in the SSVEP stimuli frequencies, as shown in figure 11.

The following observations were made based on the correlation between the SSVEP responses:

1. There was a positive correlation between the SB-SNR values and the detection accuracies, which was statistically significant ($r = 0.675$, $p = 0.004$).
2. The detection accuracy tended to drop significantly below 90% when the SNR < 22 dB.
3. The R/G stimuli no longer had superior detection accuracy with respect to the SNR compared to the R/B stimuli; however, they still yielded high SNR values.

The results showed that the SB-SNR values and detection accuracies were positively correlated.

5. Discussion

5.1. Flickering sensation towards the composite stimuli

The empirical results of this study demonstrated that alternating flickering of the R/G and R/B lights (with 180° phase shifts) produced significantly lower flickering sensations than simultaneous flickering of the component lights (figure 6 and table 4). The lower flicker perception may have been due to the absence of dark periods in the alternating flickering lights. This result is consistent with the findings of Jiang *et al* [45]. The weaker flicker perception of the alternating flickering stimuli is also in agreement with the findings of Bieger *et al* [42] regarding the comfort levels (1–7) of R/G stimuli [40]. Furthermore, alternating flickering at or above 32 Hz produced median flicker perception scores of two or lower, which was the tolerable threshold according to our criteria.

The median values of the flickering scores may have remained at two instead of dropping down to one due to the strict specification of the subjective perception scores. The standardized five-point scale required the flickering to be truly imperceptible for subjects to assign a score of one. In comparison, Jiang *et al* [45] required the composite light merely to appear, but not flicker, to claim the chromatic flicker was ‘invisible’.

With regard to the luminance, the flicker perception of the 180° relative phases was less observable with equal-luminous lights than balanced-luminous lights, which is consistent with the expectation of producing a weaker flickering sensation (section 2.2) and is also complementary to Sakurada’s green/blue (G/B) alternating flicker results [33]. The effect of luminance was highlighted with the 180° phase shift because the luminance difference of a 180° phase shift does not change as severely as that of a 0° phase shift. With regard to the colours, the flicker perception of the equal-luminous lights was slightly higher with the R/B composite stimuli than with the R/G composite stimuli. Because the short-wavelength (blue) photoreceptors had the highest spectral responsivity [52], we assumed the rectangular red and blue light pulses in the equal-luminous R/B composite stimuli had high contrast in their intensities (figure 2).

5.2. Choices of the composite colour components

The alignment between the fundamental frequencies of the SSVEP responses and the component lights may also be explained based on Hering’s opponent-process theory of colour vision [40]. According to the theory, red and green primary lights operate as excitation (+) and inhibition (−), respectively, in the receptive fields. The flickering of the opponent lights thus function antagonistically (like an ON/OFF switch) rather than in combination to produce colour vision [40]. This hypothesis, however, fails to explain why an in-phase (0°) composition of opponent lights tended to induce stronger SSVEP responses. This contradiction, along with the SSVEP responses with stronger second harmonics frequently induced by R/B composite lights with a more intense blue component than the green component in the R/G composite lights, seems to support combination as the underlying mechanism in the production of SSVEP responses towards primary coloured lights.

No statistically significant difference was detected among the foveal-SSVEP responses towards the R/G and R/B composite stimuli (table 5). These results differ from some other findings in that the strongest SSVEP responses are usually produced by red-blue composite stimuli with equal or balanced luminance, which appear as violet or purple in colour, respectively, flickering in the EEG alpha band [41]. A possible explanation of the discrepancy between these findings is that the current experiments focused on the foveal responses rather than the broad-vision responses towards high-frequency (30–40 Hz) stimuli. The results from our recent experiments [43] also showed that foveal-SSVEP responses to high-frequency monochromatic red and green lights exhibited significant SNR improvement between 25 Hz and 45 Hz.

With the exception of the R/G and R/B composite stimuli, the possibility of using G/B composite coloured lights as SSVEP stimuli with subtle flickering is reasonable based on the findings of Bieger *et al* [42] and Sakurada *et al* [33]. These results indicate that we could adopt primary coloured lights

(R/G/B) and adjust the luminance of the component colours to integrate these stimuli into commercial displays.

5.3. Robust detection of foveal-SSVEP responses towards composite stimuli

This study performed CCA between the recorded foveal-SSVEP responses and the sinusoidal reference signals. Figure 9 shows the strong differences among the correlations between the SSVEP responses with the reference signals at the flickering frequencies and those at the adjacent frequencies. These strong differences affirmed the feasibility of detecting foveal SSVEP responses induced by composite coloured stimuli.

In a real-time SSVEP-based BCI system, there is no synchronized averaging to reduce noise, but the average detection accuracies of the composite stimuli at settings of (32 Hz; 0°), (32 Hz; 180°) and (40 Hz; 0°) remained greater than 90%. In addition, the flicker perception scores of the latter two settings were acceptable because the average scores were approximately two (perceptible but not annoying).

The last trade-off settings (40 Hz; 180°) caused the least flickering sensation, but the SSVEP SB-SNR values and detection accuracies were lower. Therefore, to apply the imperceptible stimuli in interactive BDI platforms, the new CCA method with individual training data [14] should be able to improve the detection accuracy. Generally, the average accuracy ranged from 76% to 100%. These results reveal that SSVEP responses can be detectable in an online SSVEP-based BCI system using the CCA method.

6. Conclusion

With the aim of developing a new type of BDI system using flickering R/G/B lights as the visual stimuli, experiments on the effectiveness of R/G and R/B opponent coloured lights were conducted. The experimental results provided ample evidence that visual stimuli composed of R/G and R/B coloured lights flickering at 32 Hz/40 Hz can achieve a greater than 90% detection accuracy without causing annoying flickering sensations. Overall, the composite lights with 40 Hz and a 180° phase offset caused the least flickering sensations, whereas the composite lights with 0° phase offset induced the strongest SSVEP responses. Our hypothesis that the composition of the R/G and R/B opponent coloured lights with a 50% duty cycle and a phase offset of 180° is capable of inducing highly detectable SSVEP responses with little or no flickering sensations in their viewers has thus been confirmed.

These high-frequency polychromatic visual stimuli would likely find potential use in next-generation BCI systems, particularly interactive display systems. With signal processing methods such as CCA, SSVEP responses can be detected more precisely for online BCI systems. Based on this work, high-frequency polychromatic visual stimuli are promising for commercial displays. In the near future, we expect to embed the optimal imperceptible SSVEP stimuli into the LED backlight of LCDs, organic LED displays and even quantum-dot LED displays. The full integration of imperceptible SSVEP stimulation and display technologies may create next-generation interactive display systems.

Acknowledgments

This work was partially supported by grants provided by the Ministry of Science and Technology in Taiwan to the following academic research projects: NSC-102-2221-E-009-167-MY3, NSC-102-2221-E-009-168-MY3 and MOST 103-2218-E-009-012. Y Wang and T-P Jung are supported by the US Army Research Laboratory, in part, under Cooperative Agreement W911NF-10-2-0022. The authors would like to express their gratitude to the Brain Research Centre at NCTU for their technical support, to Prof Tzai-Wen Chiu for her advice and comments concerning our statistical analyses, and to Ms Chia-Ying Lee, Ms Yu-Shan Huang, Mr Wen-Hao Liu and Mr Cheng-Chi Chiu for their assistance in conducting the experiments and collecting the data.

References

[1] Huang Y-P, Lin F-C and Shieh H-P D 2011 Eco-displays: the color LCD's without color filters and polarizers *J. Disp. Technol.* **7** 630–2

[2] Holliman N S, Dodgson N A, Favalora G E and Pockett L 2011 Three-dimensional displays: a review and applications analysis *IEEE Trans. Broadcast.* **57** 362–71

[3] Wang G-Z, Huang Y-P, Chang T-S and Chen T-H 2014 Bare finger 3D air-touch system using an embedded optical sensor array for mobile displays *J. Disp. Technol.* **10** 13–8

[4] Liao L-D *et al* 2012 Biosensor technologies for augmented brain-computer interfaces in the next decades *Proc. IEEE* **100** 1553–66

[5] Lance B J, Kerick S E, Ries A J, Oie K S and McDowell K 2012 Brain-computer interface technologies in the coming decades *Proc. IEEE* **100** 1585–99

[6] Lalor E C *et al* 2005 Steady-state VEP-based brain-computer interface control in an immersive 3D gaming environment *EURASIP J. Adv. Signal Process.* **2005** 3156–64

[7] Marchesi M 2012 From Mobie to Neu: 3D animated contents controlled by a brain-computer interface *Proc. of the Virtual Reality International Conf. (Laval, France)*

[8] Adams R, Comley R and Ghoreyshi M 2009 The potential of the BCI for accessible and smart e-learning *Proc. of the Int. Conf. on Universal Access in Human-Computer Interaction (San Diego, CA)* pp 467–76

[9] Mason S G, Bashashati A, Fatourechi M, Navarro K F and Birch G E 2007 A comprehensive survey of brain interface technology designs *Ann. Biomed. Eng.* **35** 137–69

[10] Vialatte F B, Maurice M, Dauwels J and Cichocki A 2010 Steady-state visually evoked potentials: focus on essential paradigms and future perspectives *Prog. Neurobiol.* **90** 418–38

[11] Gao X, Xu D, Cheng M and Gao S 2003 A BCI-based environmental controller for the motion-disabled *IEEE Trans. Neural Syst. Rehabil. Eng.* **11** 137–40

[12] Wang Y T, Wang Y and Jung T P 2011 A cell-phone-based brain-computer interface for communication in daily life *J. Neural Eng.* **8** 025018

[13] Diez P F *et al* 2013 Commanding a robotic wheelchair with a high-frequency steady-state visual evoked potential based brain-computer interface *Med. Eng. Phys.* **35** 1155–64

[14] Nakanishi M, Wang Y, Wang Y T, Mitsukura Y and Jung T P 2014 A high-speed brain speller using steady-state visual evoked potentials *Int. J. Neural Syst.* **24** 1450019
[15] Chen X, Wang Y, Nakanishi M, Gao X, Jung T P and Gao S 2015 High-speed spelling with a noninvasive brain-computer interface *Proc. Natl Acad. Sci. USA* **112** E6058–67
[16] Chen X, Wang Y, Gao S, Jung T P and Gao X 2015 Filter bank canonical correlation analysis for implementing a high-speed SSVEP-based brain-computer interface *J. Neural Eng.* **12** 046008
[17] Wittevrongel B and Van Hulle M M 2016 Frequency- and phase encoded SSVEP using spatiotemporal beamforming *PLoS One* **11** e0159988
[18] Wittevrongel B and Van Hulle M M 2016 Hierarchical online SSVEP spelling achieved with spatiotemporal beamforming *IEEE Statistical Signal Processing Workshop (SSP) (Palma de Mallorca, Spain)* pp 1–5
[19] Wang Y, Gao X, Hong B, Jia C and Gao S 2008 Brain-computer interfaces based on visual evoked potentials *IEEE Eng. Med. Biol. Mag.* **27** 64–71
[20] Regan D 1989 *Human Brain Electrophysiology: Evoked Potentials and Evoked Magnetic Fields in Science and Medicine* (New York: Elsevier)
[21] Wu Z and Yao D 2008 Frequency detection with stability coefficient for steady-state visual evoked potential (SSVEP)-based BCIs *J. Neural Eng.* **5** 36–43
[22] Bin G, Gao X, Yan Z, Hong B and Gao S 2009 An online multi-channel SSVEP-based brain-computer interface using a canonical correlation analysis method *J. Neural Eng.* **6** 046002
[23] Wilson J J and Palaniappan R 2011 Analogue mouse pointer control via an online steady state visual evoked potential (SSVEP) brain-computer interface *J. Neural Eng.* **8** 025026
[24] Yin E, Zhou Z, Jiang J, Chen F, Liu Y and Hu D 2014 A speedy hybrid BCI spelling approach combining P300 and SSVEP *IEEE Trans. Biomed. Eng.* **61** 473–83
[25] Yin E, Zhou Z, Jiang J, Yu Y and Hu D 2015 A dynamically optimized SSVEP brain-computer interface (BCI) speller *IEEE Trans. Biomed. Eng.* **62** 1447–56
[26] Wilkins A J 1995 *Visual Stress* (Oxford: Oxford University Press)
[27] de Tommaso M, Sciruicchio V, Guido M, Sasanelli G and Puca F 1999 Steady-state visual-evoked potentials in headache: diagnostic value in migraine and tension-type headache patients *Cephalalgia* **19** 23–6
[28] Jeavons P M and Harding G F 1975 *Photosensitive Epilepsy: a Review of the Literature and a Study of 460 Patients* (London: Heinemann)
[29] Harding G F and Jeavons P M 1994 *Photosensitive Epilepsy* (London: Mac Keith Press)
[30] Fisher R S, Harding G, Erba G, Barkley G L and Wilkins A 2005 Photic- and pattern-induced seizures: a review for the epilepsy foundation of america working group *Epilepsia* **46** 1426–41
[31] Volosyak I, Valbuena D, Luth T, Malechka T and Graser A 2011 BCI demographics II: how many (and what kinds of) people can use a high-frequency SSVEP BCI? *IEEE Trans. Neural Syst. Rehabil. Eng.* **19** 232–9
[32] Chang M H, Baek H J, Lee S M and Park K S 2014 An amplitude-modulated visual stimulation for reducing eye fatigue in SSVEP-based brain-computer interfaces *Clin. Neurophysiol.* **125** 1380–91
[33] Sakurada T, Kawase T, Komatsu T and Kansaku K 2015 Use of high-frequency visual stimuli above the critical flicker frequency in a SSVEP-based BMI *Clin. Neurophysiol.* **126** 1972–8
[34] Wang Y, Wang R, Gao X, Hong B and Gao S 2006 A practical VEP-based brain-computer interface *IEEE Trans. Neural Syst. Rehabil. Eng.* **14** 234–9
[35] Garcia Molina G, Ibanez D, Mihajlovic V and Chestakov D 2009 Detection of high frequency steady state visual evoked potentials for brain-computer interfaces *Proc. of the European Signal Processing Conf. (Glasgow, Scotland)* pp 646–50
[36] Lin F-C *et al* 2012 SNR analysis of high-frequency steady-state visual evoked potentials from the foveal and extrafoveal regions of human retina *Conf. Proc.: Annual Int. Conf. of the IEEE Engineering in Medicine and Biology Society (San Diego, CA)* pp 1810–4
[37] Zao J K *et al* 2012 Human steady-state visual evoked potentials induced by high-frequency polychromatic flickering stimuli *IEEE EMB/CAS/SMC Workshop on Brain-Machine-Body Interfaces (San Diego, California, USA)*
[38] Chien Y-Y *et al* 2013 Polychromatic high-frequency steady-state visual evoked potentials for brain-display interaction *SID Symp. Digest of Technical Papers (Vancouver, Canada)* pp 146–9
[39] Cheng M, Gao X, Gao S and Xu D 2001 Multiple color stimulus induced steady state visual evoked potentials *Conf. Proc.: Annual Int. Conf. of the IEEE Engineering in Medicine and Biology Society (Istanbul, Turkey)* pp 1012–4
[40] Zhu D, Bieger J, Garcia Molina G and Aarts R M 2010 A survey of stimulation methods used in SSVEP-based BCIs *Comput. Intell. Neurosci.* **2010** 1–12
[41] Singla R, Khosla A and Jha R 2013 Influence of stimuli color on steady-state visual evoked potentials based BCI wheelchair control *J. Biomed. Sci. Eng.* **06** 1050–5
[42] Bieger J and Garcia Molina G 2010 Light stimulation properties to influence brain activity: a brain-computer interface application *Technical Note* Eindhoven, The Netherlands
[43] Chiu C-C 2014 Foveal and perifoveal SSVEP of human retina in response to high-frequency polychromatic stimuli *Master Thesis* Hsinchu, Taiwan: National Chiao Tung University
[44] Shady S, MacLeod D I A and Fisher H S 2004 Adaptation from invisible flicker *Proc. Natl Acad. Sci. USA* **101** 5170–3
[45] Jiang Y, Zhou K and He S 2007 Human visual cortex responds to invisible chromatic flicker *Nat. Neurosci.* **10** 657–62
[46] Foster M 1895 *A Text-Book of Physiology* (Philadelphia, PA: Lea Bros and Company)
[47] Goldstein E B 2009 *Sensation and Perception* (Belmont: Wadsworth/Cengage Learning)
[48] Lin F-C *et al* 2008 Dynamic backlight gamma on high dynamic range LCD TVs *J. Disp. Technol.* **4** 139–46
[49] Luo Z, Xu D and Wu S-T 2014 Emerging quantum-dots-enhanced LCDs *J. Disp. Technol.* **10** 526–39
[50] Teng F *et al* 2011 Square or sine: finding a waveform with high success rate of eliciting SSVEP *Comput. Intell. Neurosci.* **2011** 364385
[51] Ono Y A, Fuyama M, Onisawa K, Tamura K and Ando M 1989 White-light emitting thin film electroluminescent devices with stacked SrS:Ce/CaS:Eu active layers *J. Appl. Phys.* **66** 5564–71
[52] Ohta N and Robertson A 2006 *Colorimetry: Fundamentals and Applications* (Chichester: Wiley)
[53] ITU-R 2012 *Methodology for the Subjective Assessment of the Quality of Television Pictures* (Geneva: International Telecommunication Union) www.itu.int/rec/R-REC-BT.500-13-201201-I/en
[54] Mognon A, Jovicich J, Bruzzone L and Buiatti M 2011 ADJUST: an automatic EEG artifact detector based on the joint use of spatial and temporal features *Psychophysiology* **48** 229–40

[55] Bigdely-Shamlo N, Kreutz-Delgado K, Kothe C and Makeig S 2013 EyeCatch: data-mining over half a million EEG independent components to construct a fully-automated eye-component detector *Conf. Proc.: Annual Int. Conf. of the IEEE Engineering in Medicine and Biology Society (Osaka, Japan)* pp 5845–8
[56] Harris F J 1978 On the use of windows for harmonic analysis with the discrete Fourier transform *Proc. IEEE* **66** 51–83
[57] Thompson B 2000 Canonical correlation analysis *Reading and Understanding MORE Multivariate Statistics* (Washington: American Psychological Association)
[58] Gueorguieva R and Krystal J H 2004 Move over ANOVA *Arch. Gen. Psychiatry* **61** 310
[59] Montgomery D C 2008 *Design and Analysis of Experiments* (New York: Wiley)
[60] Bin G, Gao X, Wang Y, Li Y, Hong B and Gao S 2011 A high-speed BCI based on code modulation VEP *J. Neural Eng.* **8** 025015
[61] Pan J, Gao X, Duan F, Yan Z and Gao S 2011 Enhancing the classification accuracy of steady-state visual evoked potential-based brain-computer interfaces using phase constrained canonical correlation analysis *J. Neural Eng.* **8** 036027
[62] Nakanishi M, Wang Y, Wang Y-T, Mitsukura Y and Jung T-P 2014 Generating visual flickers for eliciting robust steady-state visual evoked potentials at flexible frequencies using monitor refresh rate *PLoS One* **9** e99235
[63] Won D O, Hwang H J, Dahne S, Muller K R and Lee S W 2016 Effect of higher frequency on the classification of steady-state visual evoked potentials *J. Neural Eng.* **13** 016014
[64] Hollander M, Wolfe D A and Chicken E 2013 *Nonparametric Statistical Methods* (Hoboken: Wiley)